Millimeter Wave Retrodirective Van Atta Arrays in LTCC Technology

Kamil Trzebiatowski[1], Martin Ihle[2], Benedykt Sikorski[3], Lukasz Kulas[4], Krzysztof Nyka[5]
[1] Gdansk University of Technology, Gdansk, Poland, kamil.trzebiatowski@pg.edu.pl*
[2] Fraunhofer IKTS, Dresden, Germany, martin.ihle@ikts.fraunhofer.de
[3] Gdansk University of Technology, Gdansk, Poland, benedykt.sikorski@pg.edu.pl
[4] Gdansk University of Technology, Gdansk, Poland, lukasz.kulas@pg.edu.pl
[5] Gdansk University of Technology, Gdansk, Poland, krzysztof.nyka@pg.edu.pl

***Abstract*—The millimeter wave Van Atta arrays, intended for chipless RFID applications and fabricated in LTCC technology, are presented in this paper. The arrays are designed for 24 GHz and 60 GHz bands. The method for an easy modification of the RCS characteristic by increasing the number of single-dimensional arrays, intended for increasing the RCS level, is also presented. The LTCC manufacturing process is described in detail. The fabricated arrays are characterized in an anechoic chamber and exhibit RCS levels up to -26 dBsm with a small 51 x 17 mm footprint.**

***Index Terms*—antennas, Van Atta arrays, retrodirective arrays, chipless radio-frequency identification (RFID), millimeter waves, low-temperature cofired ceramics (LTCC).**

I. INTRODUCTION

Although the concept of passive retrodirective Van Atta Arrays (VAAs) has been well known for decades, in recent years, they have emerged as a subject of increasing interest and development in the domain of wireless communication and radio-frequency identification systems. VAAs are able to reflect the incident signal directively towards the signal source, regardless of the angle of arrival (in an ideal case) [1, 2]. The amplitude, phase or polarization of the received signal can also be modified before re-transmission, by a passive or active circuit [3-5].

Due to these properties, the Van Atta arrays can be employed in a variety of fields. One such application is in extensively researched chipless radio-frequency identification (Chipless RFID) systems [3-7], in which the identification is implemented without integrated circuits in the tags. The VAAs, due to their retrodirective capabilities, could be used to realize robust, efficient, and inexpensive tags for identification and tracking, by integrating passive circuits to modulate the received signal before re-transmission [5,7].

The RFID tags are often required to work in harsh and difficult environmental conditions, like high temperature or high humidity [8] where traditional Printed Circuit Boards (PCB) may be unreliable. Moreover, at millimeter-wave frequencies, high-performance multi-layer RF substrates are required which directly translates into high costs.

In light of these challenges, Low-Temperature Co-fired Ceramic (LTCC) technology offers an attractive alternative. Multilayer ceramic-based materials (LTCC) are robust and durable, have excellent high-frequency (HF) performance, a comparatively high thermal conductivity for cooling the HF electronics and very good thermo-mechanical properties allowing for inclusion of semiconductor chips on silicon and gallium arsenide, which enables a high degree of integration. Due to these advantages, LTCC technology has proven to be one of the most suitable technology platforms for the implementation of miniaturized antennas and system-in-package devices for frequencies up to 100 GHz and above [9, 10]. However, its application in the development of VAAs, especially at higher frequencies, has not been extensively researched yet.

In this paper we present an implementation of VAAs in LTCC technology at millimeter-wave frequencies. We show the encountered challenges during the design and manufacturing processes and provide preliminary experimental results that demonstrate the feasibility and potential advantages of this approach.

II. VAN ATTA ARRAYS DESIGN

A. Base design

The investigated Van Atta arrays are based on a generic design shown in Fig. 1. The design is composed of *M* rows of one-dimensional cross-polarized Van Atta arrays (1-D VAAs), each 1-D array having *N* pairs of microstrip patches [11]. The patches in a pair are interconnected with each other in a way that the incident and re-radiated waves are of orthogonal polarization. The rows are not interconnected with each other. The design configuration and size can be changed by modifying the *M* and *N* parameters.

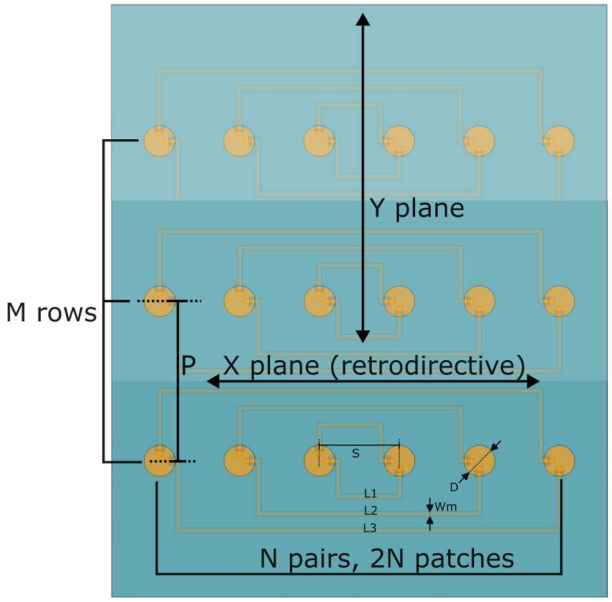

Fig. 1. Design and dimensions of the considered Van Atta arrays.

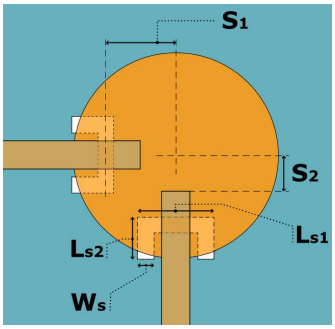

Fig. 2. Design and dimensions of a single radiating element.

The radiating elements are dual-polarized circular patches of diameter *D*, as shown in Fig. 2. The patches are fed by aperture-coupled microstrip lines through two orthogonal C-shaped slots [12], with the key dimensions of *Ls1*, *Ls2* and *Ws*. The slots are offset from the center of the patch by a distance *S1* and the feeding lines are offset from the center of the patch by a distance *S2*. The aperture coupling technique reduces unwanted radiation from the transmission lines, as they are separated from the microstrip patches by a ground plane.

The patches in the array are spaced by distance *S* equal to half the free-space wavelength λ_0 at the design frequency f_0 (24 or 60 GHz in the two presented designs). The lengths of L_i $(i = 1 \ldots N)$ differ by multiple of wavelength λ_D(in the microstrip line), so all the patches are fed in-phase. The lines have width *Wm*.

All the dimensions and their values are summarized in Table I. The presented VAAs are designed for the LTCC technology on GT951 ceramic substrate having relative permittivity $\varepsilon_r = 7.3$ in a process with two layers of thicknesses *T1* and *T2*.

TABLE I. DIMENSIONS OF THE DESIGNED ARRAYS

Dimensions and their values		
Frequency (f_0)	**24 GHz**	**60 GHz**
$\boldsymbol{\lambda_0}$	12.5 mm	5 mm
$\boldsymbol{\lambda_D}$	4.627 mm	2 mm
D	2.42 mm	0.956 mm
S	(M = 1, 4): 0.5 λ_0; (M = 2): 0.29 λ_0; (M = 3, 5): 0.82 λ_0 (central pair), 0.4λ_0 (other pairs)	0.5λ_0 = 2.5 mm
P	(M = 2): 0.87 λ_0 = 10.875 mm (M = 3, 5): 0.82 λ_0 = 10.25 mm (M = 4): 1.5 λ_0 = 18.75 mm	λ_0 = 5 mm
S1	0.39 mm	0.35 mm
S2	0.84 mm	0.15 mm
Ls1	0.73 mm	0.30 mm
Ls2	0.43 mm	0.17 mm
Ws	0.15 mm	0.08 mm
Li i = 1… N	L0 + 3$(i-1)\lambda_D$ (M = 1, 4): L0 = 11.76 mm (M = 2): L0 = 9.13 mm (M = 3, 5): L0 = 15.77 mm (central pair), L0 = 10.46 mm (other pairs)	L0 + 3$(i-1)\lambda_D$ L0 = 4.53 mm
Wm	0.36 mm	0.2 mm
T1, **T2**	0.2 mm, 0.2 mm	0.132 mm, 0.092 mm

B. Increasing the RCS by stacking the designs

Average value of the monostatic Radar Cross Section (RCS) of the designed arrays affects the maximum distance of interrogation of a VAA-based tag. It can be increased by stacking the Van Atta arrays in the Y-direction perpendicular to the retrodirective plane (see Fig. 1) [11]. The rows of 1-D elementary arrays, each comprising *N* pairs of radiating patches, are spaced by distance *P*. Doubling the number of rows *M* increases the average RCS value by around 6 dB, as presented in Fig. 3 (the higher the number of elements, the lower the RCS gain due to the increasing losses in the interconnecting lines). The RCS patterns in the Y-plane of the 60 GHz arrays are presented in Fig. 4. There are clearly visible main lobe and two strong side lobes, in contrast to the flat VAA characteristic in the X-plane. Moreover, the main beam width is decreasing with the increase of *M*. This effect is unfavorable as it reduces the maximum angle of the tag rotation in the Y-plane allowed for correct reading. The influence of this effect on the measurements is further discussed in Section IV.

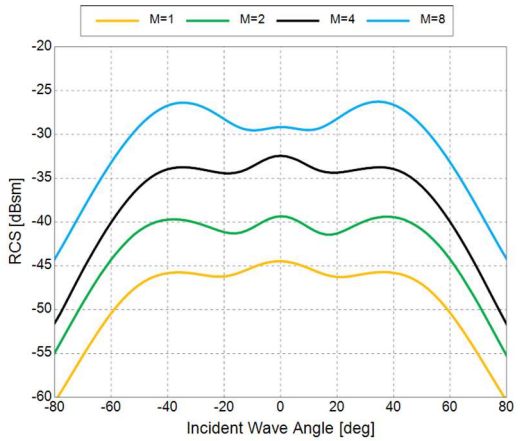

Fig. 3. The simulated RCS characteristics (in the retrodirective, X-plane, cuts) of the designed 60 GHz arrays presenting increase of the RCS value with the change of M (number of rows of 1-D arrays).

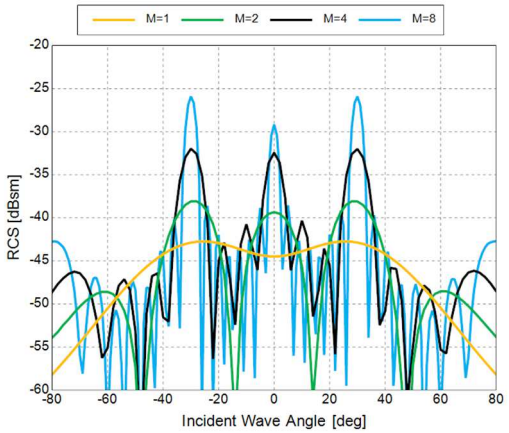

Fig. 4. The simulated RCS characteristics (in the perpendicular, Y-plane, cuts) of the designed 60 GHz arrays presenting change of the main beam shape with the change of M (number of rows of 1-D arrays).

Nine Van Atta arrays in different configurations of f_0, M and N were designed and characterized in this paper. They are summarized in Table II.

TABLE II. SIZES OF THE DESIGNED ARRAYS [MM X MM]

Configuration	**M=1, N=2**	**M=2, N=2**	**M=3, N=1**	**M=4, N=2**	**M=5, N=1**
f_0 = 24 GHz	20 x 25	24 x 18	31 x 17	83 x 26	51 x 17
Configuration	**M=1, N=3**	**M=2, N=3**	**M=4, N=3**	**M=8, N=3**	-
f_0 = 60 GHz	16 x 9	16 x 14	17 x 24	44 x 15	-

III. MANUFACTURING PROCESS

Casted DuPont ceramic soft-tapes with thicknesses of 114 µm, 165 µm and 256 µm were used for the dielectric substrate stack-ups for the designed antenna arrays. 4x4-inch LTCC tapes were used to manufacture the 24 and 60 GHz variants of VAAs. The 60 GHz antennas were manufactured on a very thin substrate stack with two layers of 165 µm and 114 µm pre-sintering thicknesses. The metallization was printed with a gold paste to prevent warpage effects during the sintering. For the 24 GHz band, a thicker stack with two 256 µm tapes and a silver paste were used. The design dimensions were increased before printing to accommodate for X-Y sintering shrinkage of the structure, which was determined in advance to be around 12.9%. In the first step, layer 1 (L1) and layer 2 (L2) were punched to insert the stacking (1 mm) and position marks (0.2 mm). This was followed by the three screen printing steps of layers L1 and L2. The ground plane with C-slot openings was printed on the topside of L1 and the feeding lines of L1 were printed on the backside. The top side of the L2 was then printed with the circular patches. A detailed view of the printed C-shaped slots is presented in Fig. 5.

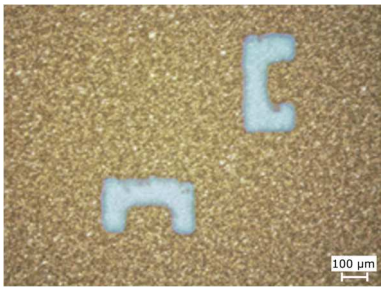

Fig. 5. Printed gold paste ground plane with C-holes with a structure width of 100 µm using a very fine resolution screen.

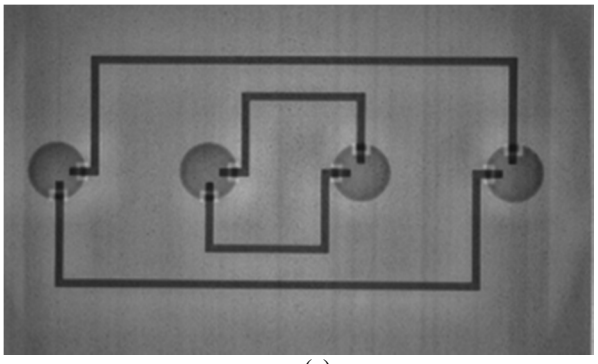

(a)

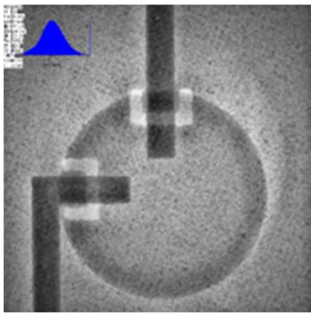

(b)

Fig. 6. (a) X-ray images of the manufactured LTCC 24 GHz Van Atta array with 4 patches, (b) a detailed view of a single radiating element.

Finally, both layers were oriented with a stacking machine and completely isostatically laminated at 200 bar and 70 °C. This was followed by sintering in a 9.5-hour oven program at a maximum of 850 °C with a debinding phase at 400 °C. During the LTCC lamination and sintering processes, the material shrank by 12.9% in x-y-direction and 20 % in z-direction. The last production step was to separate the antennas with a wafer saw.

Fig. 6 shows the X-ray images of a $N = 2$ pair 24 GHz design. Positioning of the feeding lines and the apertures slots is very precise with the help of the stacking machine. Photograph of the manufactured Van Atta arrays is shown in Fig. 7.

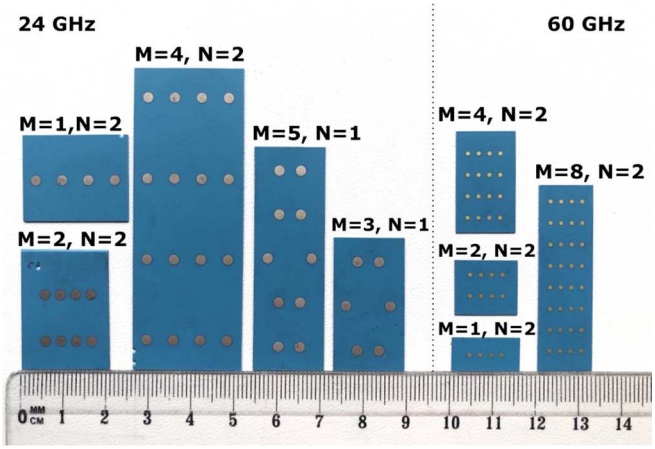

Fig. 7. A family of manufactured 24 GHz and 60 GHz Van Atta arrays.

IV. Measurements & Discussion

The measurements were performed in a millimeter-wave anechoic chamber. A cross-polarized quasi-monostatic RCS response in one plane was measured during the procedure. Quasi-monostatic means that two cross-polarized measurement antennas were used and placed close to each other, as shown in Fig. 8. The spacing between the antennas is $\Delta Y = 9$ cm and the distance between the antennas' apertures and device under test (DUT) is $\Delta X = 100$ cm.

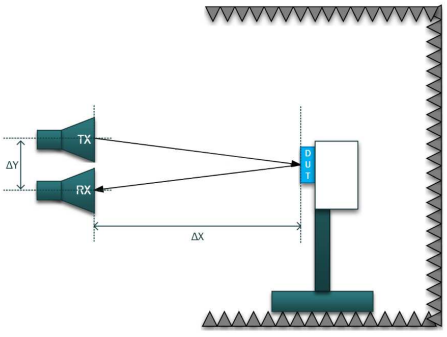

Fig. 8. Quasi-monostatic measurement setup.

A. Measurement results

The evaluation of manufactured LTCC Van Atta arrays is presented in Figures 9 and 10, where the measurement results are compared to the simulations. The absolute RCS level was calculated by comparison to a known RCS reference. The main measured parameters are summarized in Table III.

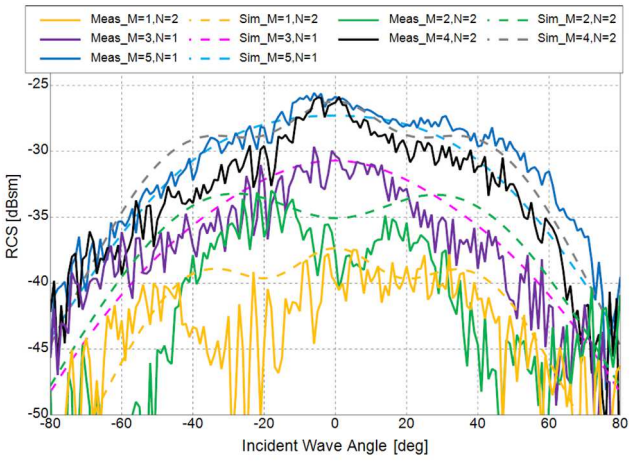

Fig. 9. Comparison of measured (*meas*) and simulated (*sim*) RCS characteristics of 24 GHz Van Atta arrays.

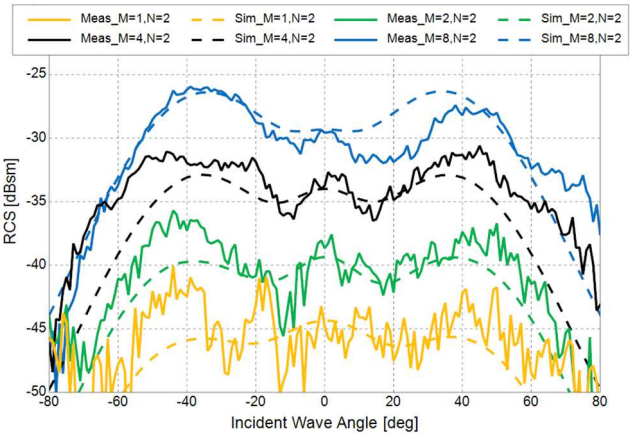

Fig. 10. Comparison of measured (*meas*) and simulated (*sim*) RCS characteristics of 60 GHz Van Atta arrays.

The measurements roughly confirm the simulated values. As it was expected, the larger the VAA, the higher the RCS level. The measured and simulated characteristics don't match exactly due to the measurement errors, such as: presence of a parallax angle between the measurement antennas, positioning errors and the deviation of the DUT's plane from the vertical plane (see subsection B).

TABLE III. MEASURED PARAMETERS OF THE MANUFACTURED VAN ATTA ARRAYS

Configuration f_0 = 24 GHz	**M=1, N=2**	**M=2, N=2**	**M=3, N=1**	**M=4, N=2**	**M=5, N=1**
Max RCS level [dBsm]	-39	-35	-33	-26	-26
-10 dB RCS angular range [°]	120	88	92	112	132
Configuration f_0 = 60 GHz	**M=1, N=2**	**M=2, N=2**	**M=4, N=2**	**M=8, N=2**	
Max RCS level [dBsm]	-40	-36	-31	-26	
-10 dB RCS angular range [°]	120	134	152	144	

B. *Measurement challenges*

The important source of measurement errors was the deviation of the measured DUT's aperture from the vertical axis (angle α), which was explained in Section II.B. A number of simulations of a 60 GHz, M = 4, N = 2 VAA were performed to assess this effect, as shown in Fig. 11.

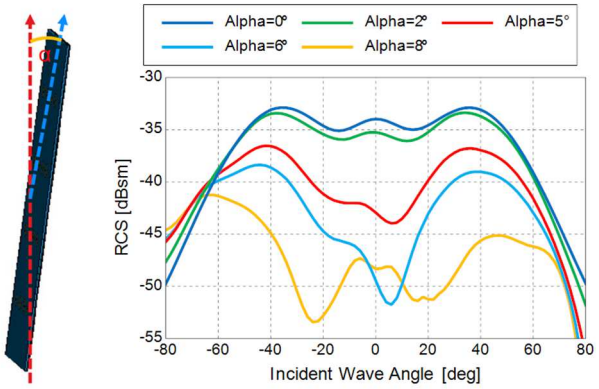

Fig. 11. Simulation of the influence of the deviation from the perpendicular plane (deviation angle α) on the measurement results.

The higher the deviation angle α, the higher the measurement error. This effect is stronger in arrays with larger number of rows M, because of their narrower main beam in the Y-plane.

V. CONCLUSION

In this paper, we have illustrated the feasibility of fabricating Van Atta arrays using LTCC technology. Their main advantages are small physical dimensions and robust design resulting in high durability in harsh environments. We have demonstrated the advantages and drawbacks of scaling a basic 1-D Van Atta array design. Increasing the number of rows along the Y-axis increases the RCS of a tag but makes it difficult to read it from a wide range of angles in the plane perpendicular to the main (retrodirective) axis, thus diminishing utility of this approach in real-world scenarios. The VAAs manufactured and presented in this study exhibit levels of RCS that are probably insufficient for practical applications. Potential solution to increase the RCS levels of the VAAs may be to design a 2-D array where patches are interconnected across both axes. Additionally, LTCC or 3-D printed lenses could be integrated with the VAA to enhance the RCS value while preserving the properties of VAAs.

ACKNOWLEDGMENT

This research was funded by the LDI MAGIC project (Reference Number: project9280), which has received funding from the M-ERA.NET 3 Partnership for research and innovation on materials and battery technologies in support of the European Green Deal. The partnership receives support from the European Union's Horizon 2020 research and innovation programme, as well as from national funding agencies from Germany (Sächsisches Staatsministerium für Wissenschaft, Kultur und Tourismus (SMWK)) and Poland (National Centre for Research and Development (NCBiR)). The document reflects only the authors' views, and the commission is not responsible for any use that may be made of the information it contains.

REFERENCES

[1] L. C. Van Atta, "Electromagnetic reflector," U.S. Patent US2908002A, 1959.

[2] E. Sharp and M. Diab, "Van Atta reflector array," *IRE Trans. Antennas Propag.*, vol. 8, pp. 436–438, 1960.

[3] S. Preradovic and N. C. Karmakar, "Chipless RFID: Bar code of the future," *IEEE Microw. Mag.*, vol. 11, pp. 87–97, 2010.

[4] C. Herrojo, F. Paredes, J. Mata-Contreras, and F. Martín, "Chipless-RFID: A review and recent developments," *Sensors*, vol. 19, no. 3385, 2019.

[5] H. Shahi, N. Masoumi, M. Mohammad-Taheri and S. Safavi-Naeini, "Dual-mode phase-conjugating/active Van Atta array design based on dual-band mixer/reflection amplifier," in *IEEE Trans. Microw. Theory Tech.*, vol. 70, no. 7, pp. 3629-3639, July 2022, doi: 10.1109/TMTT.2022.3173963.

[6] K. Trzebiatowski, M. Rzymowski, L. Kulas, and K. Nyka, "60 GHz microstrip Van Atta arrays for millimeter wave identification and localization," in *Proc. of the 2020 23rd Int. Microw. Radar Conf. (MIKON)*, Warsaw, Poland, Oct. 5–8, 2020, pp. 132–135.

[7] K. Trzebiatowski, M. Rzymowski, L. Kulas, and K. Nyka, "Simple millimeter wave identification system based on 60 GHz Van Atta arrays," *Sensors*, vol. 22, no. 24, p. 9809, Dec. 2022, doi: 10.3390/s22249809.

[8] V. Franchina, A. Ria, A. Michel, P. Bruschi, P. Nepa and A. Salvatore, "A compact UHF RFID ceramic tag for high-temperature applications," *2019 IEEE Int. Conf. RFID Tech. Appl. (RFID-TA)*, Pisa, Italy, 2019, pp. 480-483, doi: 10.1109/RFID-TA.2019.8892217.

[9] M. Ihle, S. Ziesche, C. Zech and B. Baumann, "Compact LTCC packaging and printing technologies for sub–THz modules," in *Proc. of the 2018 7th Electron. System-Integr. Tech. Conf. (ESTC)*, Dresden, Germany, 2018, pp. 1-4, doi: 10.1109/ESTC.2018.8546400.

[10] A. Bhutani *et al*., "122 GHz aperture-coupled stacked patch microstrip antenna in LTCC technology," in *Proc. of the 2016 10th Eur. Conf. Antennas Propag. (EuCAP)*, Davos, Switzerland, 2016, pp. 1-5, doi: 10.1109/EuCAP.2016.7481147.

[11] X. -F. Li, Y. -L. Ban, Q. Sun, Y. -X. Che, J. Hu and Z. Nie, "A compact dual-band Van Atta array based on the single-port single-band/dual-band antennas," in *IEEE Antennas Wirel. Propag. Letters*, vol. 22, no. 4, pp. 888-892, April 2023, doi: 10.1109/LAWP.2022.3227577.

[12] K. Trzebiatowski, W. Kalista, M. Rzymowski, Ł. Kulas and K. Nyka, "Multibeam antenna for Ka-band CubeSat connectivity using 3-D printed lens and antenna array," in *IEEE Antennas Wirel. Propag. Letters*, vol. 21, no. 11, pp. 2244-2248, Nov. 2022, doi: 10.1109/LAWP.2022.3189073.